

SYNTHESIS AND TRIBOLOGICAL PROPERTIES OF Ti-DOPED WSe₂ NANOFLLAKES

K. ZHANG^a, H. P. LI^a, Q. SHI^{a,c}, J. XU^a, H. T. ZHANG^a, L. CHEN^a, C. S. LI^{a,b*}

^a*School of Materials Science and Engineering, Jiangsu University, Zhenjiang 212013, Jiangsu Province, China*

^b*School of Materials Science and Engineering Jiangsu University, Key Laboratory of Tribology of Jiangsu Province, ZhenJang 212013, China*

^c*ZhenJiang vocational Technical college ZhenJiang 212016, China*

The Ti-doped WSe₂ nanoflakes have been successfully prepared via solid-state thermal (700°C) reaction between micro-sized Ti, W with Se powders under inert atmosphere in a closed reactor and characterized by X-ray diffractometer (XRD), scanning electron microscopy (SEM) and transmission electron microscopy (TEM). The results indicated the morphologies of Ti-doped WSe₂ changed with the doping of Ti powders. And the sizes of crystallites evidently reduced while the contents of dopant increased within a certain limit (1at.%–5at.%). The tribological properties of the as-prepared products as additives in paraffin base oil were investigated by UMT-2 multi-specimen tribotester. The lubrication properties of base oil is improved by both WSe₂ and Ti-doped WSe₂. Furthermore, the lubrication properties of Ti-doped WSe₂ are better than those of pure WSe₂ in HVI500 base oil, which could be attributed to their thin laminated structure and the Ti dopant.

(Received November 25, 2014; Accepted February 6, 2015)

Keywords: Nanoflakes, Ti-doped WSe₂, Solid-state reaction, Tribological properties

1. Introduction

The transition metal dichalcogenides MX₂ (M=Mo, W, Nb; X=S, Se) crystals have a hexagonal layered structure[1-4]. It is well known that transition metal dichalcogenides have a sandwich interlayer structure formed by stacking of the X-M-X layers, which is similar to the graphite structure. The layers are held together by weak van der Waals forces and easily cleaved. Owing to this unique structure, they were shown to exhibit very good behavior with numerous potential applications, such as solid lubricant, semiconducting, photovoltaic solar cells, superconducting[5-7], etc. Particularly in the field of lubrication, it was revealed that these nanoflakes perform very effectively as additives in lubrication fluids[8-12] or powder composites improves the tribological conditions of the contact pairs[13-14], which made them become one of the focuses of research.

Various methods were put forward to improve the properties of transition metal dichalcogenides. The doping of transition metal dichalcogenides provides a practical path to tailor their physical and chemical properties by creating new states that modify their electronic structure[15]. For example, Johnny Tannous et al[16]. fabricated the Mo_xW_{1-x}S₂ inorganic fullerenes by means of MOCVD found that the particles size and crystallinity affects the tribological performance. L.Rapoport et al.[17] discovered that Re-doped fullerene-like MoS₂ nanoparticles provides ultra-low friction coefficient and very low wear rate. Scharf et al[18]. reported the friction behavior of Ti-doped WS₂ nanocomposite thin films, which displayed a lower friction coefficient at room temperature and longer lifetimes for high temperature(500°C) friction tests.

*Corresponding authors: l_changsheng@yahoo.com

In recent works[19, 20, 26], we reported the successful experimental of Mo-doped WSe₂ nanoflakes with thinner and smaller structures by a facile solid-state reaction, which showed a lower friction coefficient as additives in the HVI500 base oil compared with pure WSe₂. In this study, the Ti-doped WSe₂ nanoflakes had been successfully synthesized by a facile solid-state reaction. The products were characterised by an X-ray diffractometer (XRD), and scanning electron microscopy (SEM). Moreover, experiments at different sliding distances were performed in the boundary-lubrication regime under a constant normal load and sliding velocity on a ball-on-disc tribotester, and the results were compared to the reference HVI500 base oil and pure WSe₂. It showed that the introduction of Ti dopant led to an obvious size reduction and variation in morphologies. Then, the Ti-doped WSe₂ nanoflakes exhibit an excellent anti-wear and friction reducing properties.

2. Experimental

2.1 Synthesis of WSe₂ and Ti-doped WSe₂ nanoflakes

Elemental selenium, titanium and tungsten powders were purchased from Shanghai Chemical Reagent Co. Ltd. (Shanghai, China). All chemical reagents were of analytic purity and used directly without any further purification. Before to the preparation of nano-crystals, the powders of the elements were mixed in the ball-milling pot that aerated with Argon and mechanically milled at 300rpm (rotation per minute) for 8 hours then sealed in silica glass tubes under secondary vacuum (10^{-6}) at a certain ratio. After sealing, the ampoule(sealed tube) was set in vacuum furnace. The temperature of the tube furnace was raised from room temperature to 700 °C at a rate of 7 °C/min and the temperature was maintained at 700 °C for 1h. Subsequently the ampoule was gradually cooled to room temperature, then the as-prepared powder was obtained. Summary of the samples doped with different amounts of Ti powder are shown in table 1.

Power X-ray diffraction (XRD) patterns of the products are performed on a D8 advance(Bruker-AXS) X-ray Diffractometer with Cu K α =1.5418 Å radiation. The XRD data were recorded in the 2 θ -range 10-80° at a scan speed of 5°min⁻¹. The morphologies and structures of the samples are characterized by scanning electron microscopy(SEM, JEOL JXA-840A) and transmission electron microscopy(TEM) with a Japan JEM-100CX II transmission electron microscope.

Table 1 Summary of the samples doped with different amounts of Ti powder.

Sample	Ti-containing	Ti:W:Se/mole ratio	Crustallite sizes/(002) plane
A1	0	0:100:210	562nm
A2	1%	1:99:210	491 nm
A3	3%	3:97:210	260 nm
A4	5%	5:95:210	390 nm

2.2 Tribological Properties of Ti-doped WSe₂ Nanoflakes as Lubrication Additive

Different mass fractions of Ti-doped WSe₂ nanoflakes were dispersed in the HVI500 base oil via 2h ultrasonication without any active reagent. The friction and wear testing was carried out using the UMT-2 ball-on-plate friction and wear tester. The friction tests of oil mixed with pure WSe₂ and Ti-doped WSe₂ respectively were conducted under different loads and sliding speeds. The material of upper sample is 440C stainless steel ball with a diameter of 9mm, hardness of 62HRC, and the counterpart is 45 steel disc of Φ 40mm \times 3mm in size. The friction coefficient was automatically recorded during the contact friction. The morphology of the wear scar was examined by a JSM-5600LV scanning electron microscope (SEM).

3. Results and discussion

3.1 Characterizations of Ti-doped WSe₂

The XRD patterns of WSe₂ and Ti-doped WSe₂ is illustrated in figure 1. All the peaks could be readily indexed to those of the hexagonal phase (p63/mmc (194) space group) of WSe₂ with lattice constants $a=3.286 \text{ \AA}$ and $c=12.983 \text{ \AA}$ (PDF No.38-1388). No characteristic peaks of other impurities are detected in the XRD pattern, indicating that Ti-doped WSe₂ with high purity can be obtained under current synthesis conditions. The figure 1.a pure WSe₂ (002) peak displayed a prominent signal, which indicated a well-stacked layered structure. It can be seen from the figure that the intensity of the diffraction peaks exhibited obvious reduced and widen with the introduction of Ti reached 1 at.% - 3 at.%, the results indicate that the size of nanoflakes is decreased. When the content of Ti powder is increased to 5at.%, the intensity of the diffraction peaks and the crystallite sizes are increased compared with 3at.%. The crystallite sizes ((002) plane) of Ti-doped are listed in Table 1. Which can confirmed that the following SEM observation.

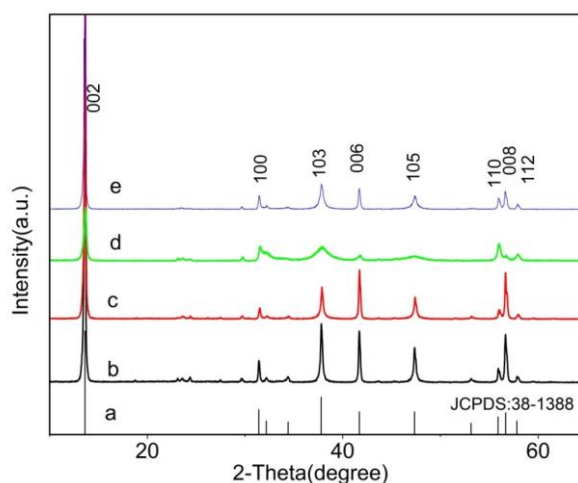


Fig.1 X-ray powder diffraction patterns of Ti-doped (a: standard PDF WSe₂, b: pure WSe₂, c: Ti-doped (1at.%) WSe₂, d: Ti-doped (3at.%) WSe₂, e: Ti-doped (5at.%) WSe₂) prepared at 700 °C for 1 h.

The size and morphology of WSe₂ and Ti-doped WSe₂ products were investigated by SEM and TEM. Figure 2 shows typical SEM images of the WSe₂ and Ti-doped WSe₂ nanoflakes. Figure 2a shows that the as-prepared pure WSe₂ crystallites were hexagonal flake-shaped with the diameters is about 1-5 μm , and the thickness varying between 0.2 and 0.35 μm . When the content of Ti-doped is 1at.% (figure 2b), many nanoflakes began to aggregate together. And most of this nanoflakes were smaller (the diameters is about 300nm to 1 μm) than pure WSe₂. With the titanium content increased to 3at.%, the nanoflakes assemble together, imbricating into a peculiarly tower-shaped morphology (figure 2c). When Ti-doped is 5at.% (figure 2d), the as-prepared Ti-doped WSe₂ began from the tower-shaped to the fluffy hexagonal nanoflakes structure. From the magnified SEM images (figure 2d), it is clearly found that the sizes of the nanoflakes are about 100-200 nm in diameter and 30-50nm in thickness, is smaller and thinner than pure WSe₂. The conclusion is extremely in accordance with the results of XRD calculated with the FWHM of (002) plane (table 1).

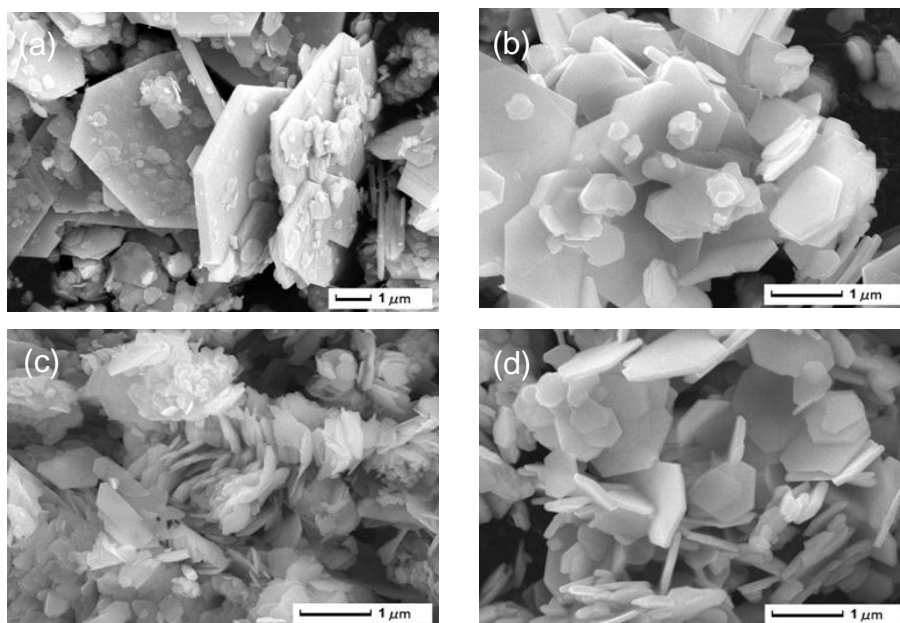


Fig.2 SEM images of WSe₂ prepared with: (a) pure WSe₂; (b) Ti-doped with 1at%; (c) Ti-doped with 3at%; (d) Ti-doped with 5at%.

From the literatures [21-23] reported growth mechanism of MoS₂ and WSe₂. We know that under the high temperature conditions, Se quickly evaporated and simultaneously reacted with W. This rapid reaction might lead to super saturation and fast nucleation. Thus, numerous nuclear of WSe₂ were initially formed in the vapor phase. When the initial clusters grew to the critical size, they began to form crystal flakes. For Ti-doped WSe₂, this observation could be referred to the fact that the activity of Ti is higher than W. When the Ti doped may result in easier nucleation and more preferred orientation. Especially the Ti content is 3at.% and 5at.% that may easier lead to a noticeable aggregation with the collisions between W and Se atoms[24, 25].

The morphology and structure of the as-synthesized WSe₂ and Ti-doped WSe₂ nanoflakes were further characterized using TEM. Figure 3a shows a TEM and SAED pattern of the typical WSe₂ nanoflakes. The prepared WSe₂ are micro size flakes and the inserted selected area electron diffraction pattern in figure 3a further indicates the single crystalline nature of the hexagonal flake, which is consistent with the SEM images. Figure 3b is the TEM image of Ti-doped (5at.%) WSe₂ flakes shows hexagonal flake shaped with the length of about 200 nm. The nanoflakes are smaller hexagonal crystal structure, which is in good agreement with the SEM observations of the nanoflakes.

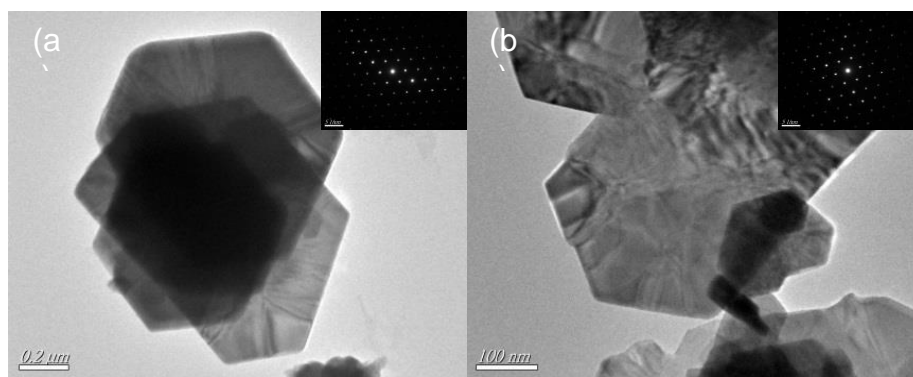


Fig.3 (a) TEM and SAED pattern of WSe₂ flakes. (b) TEM and SAED pattern of Ti-doped (0.5%) WSe₂.

3.2 Effect of Ti-doped WSe₂ on lubrication properties

Fig. 4 shows the effect of HVI500 basic oil and the base oil containing 5 wt.% A1 – A4 samples at the loads of 20N under different speeds (100~500 rpm) for 20min. Primarily, it can be observed that all stoichiometric variations of Ti-doped WSe₂ considerably reduce friction coefficient compared to the HVI500 basic oil. Especially, the base oil with 5at.%Ti-doped WSe₂ nanoflakes have lower friction coefficient compared with other content Ti-doped WSe₂ of the friction. At the load of 20N, the friction coefficient decreased as the sliding velocity increased. This can be attributed to the fact that the lubrication of WSe₂ and Ti-doped WSe₂ as oil additive is mainly dependent on the formation of tribofilm in the friction process. With the increase of sliding velocity, the shear stress increased, which is beneficial for the formation of tribofilm. The figure 5 shows the friction coefficient at 300rpm under different loads (5N, 10N, 20, 40, 60, 80N). The friction coefficient of the HVI500 basic oil containing WSe₂ and Ti-doped WSe₂ nanflakes is lower than that of basic oil at all the load. At the same time, the friction coefficient of base oil without any additive is increased sharply with the load increasing. But the friction coefficient of basic oil containing Ti-doped nanoflakes is lower and more stable than that of WSe₂.

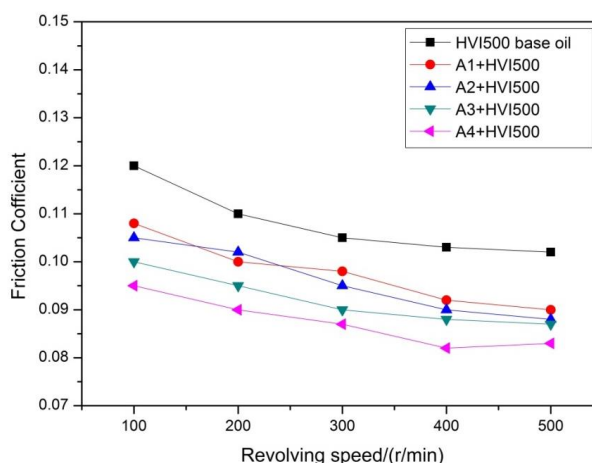


Fig.4 Variation of friction coefficient at the load of 50N under diverse speeds for the HVI500 base oil and the HVI500 base oil containing 5wt.% A1, A2, A3, A4.

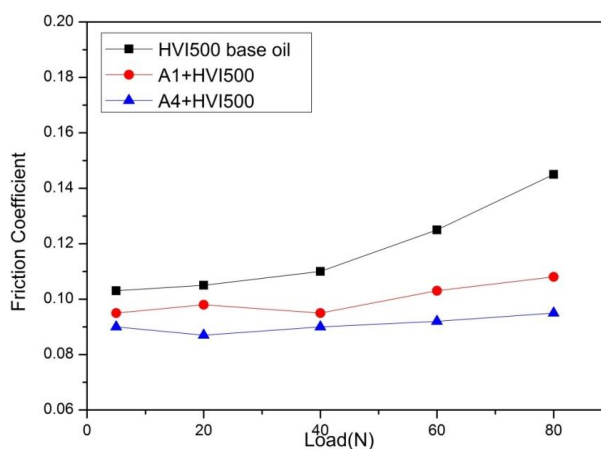


Fig.5 Variations of friction coefficient of the paraffin base oil and the base oil containing 5wt.%A1, A with increasing load at 300rpm for 20min.

After tribological tests, the wear scar surfaces of the steel discs were analyzed by SEM (figure 6). It can be observed that the worn surface of the steel disc lubricated by HVI500 base oil

was evidently rough with many thick and deep furrows (figure 6a). However, the worn scar surfaces of the base oil containing the WSe_2 nanoflakes was flat and smooth than figure 6a. At the same time, a relative flat and smooth wear scar (figure 6c) was obtained under the lubrication of the HVI500 base oil containing Ti-doped (0.5) WSe_2 , and its furrows are smoother compared with lubricated by the HVI500 base oil with WSe_2 . According to the previous results, the tribological properties of the base oil containing Ti-doped(0.5) WSe_2 as additive in HVI500 base oil have excellent friction-reducing and anti-wear properties than that with WSe_2 .

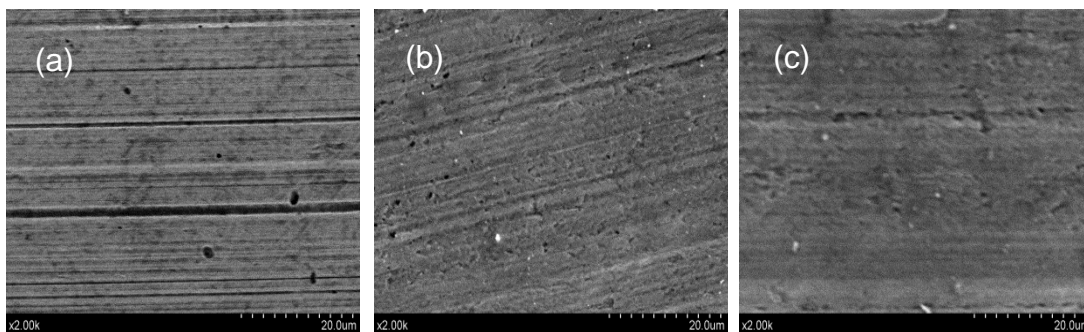


Fig.6 SEM images of the worn surface of the steel disc under a constant load of 20N after 20min: (a) lubricated with the HVI500 base oil; (b) with the HVI500 base oil containing 5wt.% WSe_2 ; (c) with the HVI500 base oil containing 5wt.% A4 shows that the solid lubricating film can well protect the integrity of the film and enhance the capability of resist compression.

From the above results, WSe_2 and Ti-doped WSe_2 nanoflakes as lubrication additive could improve tribological properties of the HVI500base oil. In this study, the effect WSe_2 and Ti-doped WSe_2 nanoflakes as lubrication additive could be attribute to the molecule bearing mechanism of sliding friction and rolling friction between the rubbing surfaces. When the load increased, the stability of lubricant film reduced, but with the load keeps adding up, the lubricant film became unstable and easily splintered. The friction coefficient became high at high contact pressure, as shown in figure 5. At the same time, with the increase of rotating speed, the friction coefficient became decreased because of the tribofilm became more and more stable (figure 4). The incorporation of Ti atoms reduces the strength of Van der Waals gap between the Ti-doped WSe_2 planes leading to easier stripping and the Ti play the part of separation role [20]. The Ti-doped(0.5) WSe_2 gradual exfoliation and transfer of molecular sheets onto the asperities of the reciprocating surfaces on high contact pressure, the smaller size of Ti-doped(0.5) WSe_2 nanoflakes more easily penetrate into the rubbing surfaces resulting in an improvement of the friction coefficient. In this work, we considered that the sliding of the Ti-doped WSe_2 nanoflakes in the interface between rubbed surfaces played a main role for the super tribological properties.

4. Conclusions

In this paper we successfully prepared WSe_2 and Ti-doped WSe_2 nanoflakes by a solid phase synthesis method. The SEM, TEM images and XRD analysis both reveal that the existence of Ti-plays an important role in refining the size and the morphology of WSe_2 nanoflakes. Compared with pure WSe_2 , the HVI500 base oil with the addition of Ti-doped WSe_2 nanoflakes showed the better lubrication properties. The Ti-doped nanoflakes with thinner and smaller morphologies could form a more stable tribofilm on the rubbing surface exhibit a excellent anti-wear and friction reducing properties.

Acknowledgements

This work was financially supported by National Natural Science Foundation of China (51275213, 51302112), the Jiangsu National Nature Science Foundation (BK2011534, BK2011480), the Jiangsu Industry-University-Research Joint innovation Foundation (BY213065-05, BY213065-06) and Scientific and Technological Innovation Plan of Jiangsu Province in China (Grant Nos. CXLX13_645).

References

- [1] W. A. Abdallah, E. Nelson, *J. Mater. Sci.* **40**, 2679 (2005).
- [2] V. G. Pol, S. V. Pol, and A. Gedanken, *J. Nano Res.* **3**, 15 (2008).
- [3] H. Q. Shi, X. D. Zhou, Y. S. Lin, and X. Fu, *Mater. Lett.* **62**, 3649 (2008).
- [4] N.D. Boscher, C.J. Carmalt, I.P. Parkin, *J. Mater. Chem.* **16**, 122 (2006).
- [5] T. Tsuneta, T. Tushima, K. Inagaki, T. Shibayama, S. Tanda, S. Uji, M. Ahlskog, P. Hakonen, M. Paalanen, *Curr. Appl. Phys.* **3**, 473 (2003).
- [6] Z. Salman, D. Wang, K.H. Chow, M.D. Hossain, S.R. Kreitzman, T.A. Keeler, C.D.P. Levy, W.A. MacFarlane, R.I. Miller, G.D. Morris, T.J. Parolin, H. Saadaoui, M. Smadella, R.F. Kiefl, *Phys. Rev. Lett.* **98**, 167001 (2007).
- [7] F. Soto, H. Berger, L. Cabo, C. Carballeira, J. Mosqueira, D. Pavuna, P. Toimil, F. Vidal, *Physica C* **460**, 789 (2007).
- [8] L. Rapoport, Y. Bilik, Y. Feldman, M. Homyonfer, S.R. Cohen, R. Tenne, *Nature* **387** (1997).
- [9] L. Cizaire, B. Vacher, T. Le Mogne, J.M. Martin, L. Rapoport, A. Margolin, R. Tenne, **160**, 282 (2002).
- [10] L. Joly-Pottuz, F. Dassenoy, M. Belin, B. Vacher, J.M. Martin, N. Fleischer, *Tribol. Lett.* **18**, 477 (2005).
- [11] A. Moshkovith, V. Perfiliev, A. Verdyan, I. Lapsker, R. Popovitz-Biro, R. Tenne, *Tribol. Int.* **40**, 117 (2007).
- [12] J. Tannous, F. Dassenoy, A. Bruhács, W. Tremel, *Tribol. Lett.* **37**, 83 (2010).
- [13] L. Rapoport, M. Lvovsky, I. Lapsker, V. Leshchinsky, Y. Volovik, Y. Feldman, A. Margolin, R. Rosentsveig, R. Tenne, *Nano. Lett.* **1**, 137 (2001).
- [14] L. Rapoport, M. Lvovsky, I. Lapsker, W. Leshchinsky, Y. Volovik, Y. Feldman, R. Tenne, *Wear.* **249**, 150 (2001).
- [15] D. J. Norris, A. L. Efros, and S. C. Erwin, *Science.* **319**, 1776 (2008).
- [16] J. Tannous, F. Dassenoy, A. Bruhács, W. Tremel, *Tribol. Lett.* **37**, 83 (2009).
- [17] L. Rapoport, A. Moshkovich, V. Perfilyev, A. Laikhtman, I. Lapsker, L. Yadgarov, *Tribol. Lett.* **45**, 57 (2011).
- [18] T. W. Scharf, A. Rajendran, R. Banerjee, F. Sequeda, *Thin Solid Films* **517**, 5666 (2009).
- [19] W. J. Li, L. F. Hu, M. Z. Wang, H. Tang, C. S. Li, J. Q. Liang, Y. Jin, *Cryst. Res. Technol.* **47**, 878 (2012).
- [20] X. H. Zhang, H. Tang, C. S. Li, S. Chen, *Chalcogenide Lett.* **10**, 403 (2013).
- [21] X. L. Li, Y.D. Li, *Chem. Eur. J.* **9**, 2726 (2003).
- [22] X. L. Li, J.P. Ge et al., *Chem. Eur. J.* **10**, 6163 (2004).
- [23] J. H. Yang, H. X. Yao, Y. Q. Liu, Y. J. Zhang, *Nanoscale Res Lett.* **3**, 481 (2008).
- [24] J. S. Santos, F. Trivinho-Strixino, and E. C. Pereira, *Corros. Sci.* **73**, 99 (2013).
- [25] A. Khaleel, M. Nawaz, S. Al-Hadrami, Y. Greish, and T. Saeed, *Microporous Mesoporous Mater* **168**, 7 (2013).
- [26] Q. SHI, H. Tang, H. Zhu, G. Tang, K. Zhang, H. Zhang, C. Li, *Chalcogenide Lett.* **11**, 199 (2014).